JOURNAL OF SPACECRAFT AND ROCKETS
Vol. 33, No. 6, November–December 1996

Nonlinear Dynamical Characteristics Analysis of Tethered Subsatellite in the Presence of Offset

Xingyu Gou,* Xingrui Ma,† and Chengxun Shao‡
Harbin Institute of Technology, Harbin 150001, People's Republic of China

The tethered satellite system has potential applications in space engineering, such as retrieval of subsatellites, experiments in microgravity sciences, and radiation measurement in outer space. Nonlinear dynamical characteristics of a tethered subsatellite in the presence of offset are considered. The dynamic equations of the tethered satellite system are derived by using a Lagrangian formulation, in which the main satellite (Space Shuttle) moves in an elliptical orbit and the tethered subsatellite vibrates in the presence of air drag. Linear and nonlinear vibrations and the influence of the tether attachment to the Space Shuttle on the motion of the tethered subsatellite are discussed. The dynamic equations of the tethered satellite system are analyzed theoretically, and some insights are obtained. Finally, numerical results on the tethered subsatellite in different phases of motion are given, and comparisons are made. It has been found that a linear model cannot be used for retrieval, especially in the presence of an offset.

Nomenclature

A = effective area normal to velocity V, m^2
a_0 = half length of the major axis of the elliptical orbit, m
C_d = drag coefficient
e = eccentricity of the orbit
F = aerodynamic force on system, N
i = inclination of the orbital plane to the equatorial plane, deg
i, j, k = unit vectors along $\mathbf{S}x$, $\mathbf{S}y$, $\mathbf{S}z$ axes
l = deployed tether length, m
m_s = mass of the tethered subsatellite, kg
Q_i = generalized forces corresponding to three degrees of freedom
R = polar radial vector from the Earth's center to the system center of mass, m
R_* = vector from point **B** to **O** as shown in Fig. 2, m
s = tether attachment offset on the Space Shuttle, m
t = time, s
V = velocity of the system relative to the atmosphere, m/s
V_a = velocity of atmosphere due to its rotation about the Earth's axis, m/s
V_i = inertial velocity of the mass center of the system, m/s
V_s = absolute velocity of the subsatellite in the inertial frame **EXYZ** at the Earth's center, m/s
α = path angle of the Space Shuttle relative to the local horizontal, deg
θ = true anomaly, rad
θ_p = argument of the perigee, rad
$\bar{\theta}$ = $\theta + \theta_p$
μ = attractive force coefficient of the Earth, m$^3 \cdot$ s^{-2}
ρ = density of the air, kg $\cdot$ m^{-3}
σ = angular velocity vector of the Earth's atmosphere, s^{-1}
τ = tension of the tether, N
ϕ = in-plane swing angle of the tethered subsatellite, deg
ψ = out-of-plane swing angle of the tethered subsatellite, deg
$\dot{}$, $'$ = differentiation with respect to t and θ, respectively

Received June 20, 1995; revision received Nov. 12, 1995; accepted for publication March 25, 1996.

*Doctoral Student, Department of Astronautics and Mechanics, P.O. Box 137.
†Professor of General Mechanics, School of Astronautics, P.O. Box 333.
‡Professor of General Mechanics, Department of Astronautics and Mechanics, P.O. Box 137.

Introduction

THE concept of a tethered satellite system appeared in the literature as early as the 1950s and 1960s,[1] mainly in relation to early needs such as retrieval of stranded astronauts, experiments in microgravity science, radiation measurements in outer space, etc.[2,3] More recently, it has been found that this kind of system could be used more widely. For instance, some sophisticated scientific experiments aimed at magnetic and aerothermodynamic measurement can be conducted[4,5]; payloads can be deployed to a new orbit; a satellite that has deteriorated can be retrieved[6,7]; electricity can be generated with an electrodynamic tether cutting the global magnetic field[8]; and so on. Thus the tethered satellite system has become an interesting topic in space research. It is believed that the day is coming when such a system will be used in practical space engineering.

Because of the complexity of the problem, the dynamic equations of the tethered satellite system have usually been linearized.[9–11] In this paper, by means of a Lagrangian formulation, the nonlinear dynamic equations of the attitude motion of the system are developed. The simple cases are discussed in depth, and some insights are gained. A significant amount of numerical simulation is also presented. Linear and nonlinear results are compared to indicate when linearization is feasible. In addition, the influence on the motion of the tethered satellite of an offset s of the tether's attachment to the Space Shuttle has been studied.

Dynamical Equations of the Attitude Motion of the System

Modeling

As many research workers have pointed out, in its utmost generality, the dynamical problem of the tethered satellite system is quite challenging.[12,13] In this paper, the motion of the subsatellite attached to the Space Shuttle is discussed. The system is composed of the Space Shuttle, a subsatellite, and a connective tether. Figure 1 shows the dynamic model, where $\mathbf{O}xyz$ is the orbital frame. The $\mathbf{E}x$ axis is along the radial line connecting the Earth's center to the system's center of mass; $x\mathbf{O}y$ is the orbital plane; the y axis is along the local vertical, and the z axis completes the three-orthogonal-axis frame.

In our model, the following assumptions are made: 1) the system moves in an elliptical orbit; the attitude motion and the orbital motion are considered uncoupled; the subsatellite is regarded as a mass point; the mass of the Space Shuttle is much larger than that of the subsatellite (the mass center of the system, therefore, is always coincident with that of the Space Shuttle); 2) the tether is attached to point **A** of the Space Shuttle on its longitudinal axis with an offset s relative to the mass center of the system; 3) the attitude motion consists of in-plane and out-of-plane librational motions; other elastic vibrations superposed on the attitude motion are considered

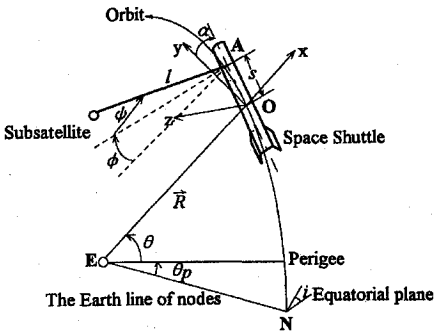

Fig. 1 Sketch of the dynamical model of the tethered satellite system.

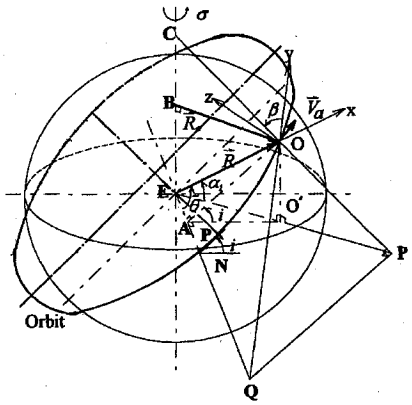

Fig. 2 Sketch of the development of the relative velocity V.

insignificant and negligible; 4) the mass of the tether is neglected; and 5) other small external forces, except for air drag, are not taken into account.

Consequently, only three degrees of freedom of the system attitude motion are considered in this paper, namely, the deployed tether length and the in-plane and out-of-plane swing angles of the tethered subsatellite.

We will consider air drag first. The aerodynamic force on the system can be expressed as

$$\boldsymbol{F} = -\tfrac{1}{2}C_d\rho A\boldsymbol{V}|\boldsymbol{V}| \tag{1}$$

where ρ changes quickly with the altitude,[14] and since the Space Shuttle usually moves in an orbit at an altitude greater than 180 km, the air drag on the Space Shuttle can be neglected.

The relative velocity of the subsatellite depends on the inertial velocity of the mass center of the system, the velocity of the atmosphere due to its rotation about the Earth's axis, and the velocity of the subsatellite relative to the mass center of the system. The last velocity is comparatively small. Therefore

$$\boldsymbol{V} = \boldsymbol{V}_i - \boldsymbol{V}_a \tag{2}$$

The geometric relationship for the relative velocity is shown in Fig. 2, where the plane **OPQ** is the tangent plane of the celestial sphere at point **O**, which represents the system; **O′** is the projection of **O** on the equatorial plane; x**O**z and **PCE** represent the same plane; and the line segment **BO** is parallel to **EO′**, which is the projection of the vector $\boldsymbol{R}$ on the equatorial plane. From Fig. 2, it is obvious that

$$\boldsymbol{V}_i = \dot{R}\boldsymbol{i} + R\dot{\theta}\boldsymbol{j} \tag{3}$$

$$\boldsymbol{V}_a = \boldsymbol{\sigma} \times \boldsymbol{R}_* \tag{4}$$

The expression for the relative velocity is found to be

$$\boldsymbol{V} = \dot{R}\boldsymbol{i} + R(\dot{\theta} - a\sigma\sin\beta)\boldsymbol{j} + (a\sigma R\cos\beta)\boldsymbol{k} \tag{5}$$

where a, α_1, and β are as follows:

$$a = \sqrt{1 - \sin^2\tilde{\theta}\sin^2 i}$$

$$\alpha_1 = \arccos a \cdot \operatorname{sign}(\sin\tilde{\theta}) \tag{6}$$

$$\beta = \arccos\frac{\tan\alpha_1}{\tan\tilde{\theta}}$$

Second, the path angle of the Space Shuttle relative to the local horizontal can be expressed as

$$\tan\alpha = \frac{\dot{R}}{R\dot{\theta}} = \frac{e\sin\theta}{1 + e\cos\theta} \tag{7}$$

Since $e \ll 1$ and α is generally small, we obtain

$$\alpha \approx e\sin\theta \tag{8}$$

Dynamical Equations

The Lagrangian formulation is utilized in this subsection to obtain the expression for the kinetic energy of the subsatellite where only the three degrees of freedom l, ϕ, ψ of the subsatellite need to be considered. Figure 3 will help us to develop the formula for the absolute velocity of the subsatellite in the inertial frame **EXYZ** at the Earth's center. In Fig. 3, **O**xyz is again the orbital frame. The frame **A** $x_a y_a z_a$ is attached to the Space Shuttle at the point **A**, and its orientation is specified by the value of the path angle α about the **O**x axis. Applying a series of kinetic relationship, we obtain

$$\begin{aligned}\boldsymbol{V}_s = [&-\dot{l}\cos\psi\cos\phi + l\sin\psi\cos\phi\cdot\dot{\psi}\\ &+ l\cos\psi\sin\phi\cdot(\dot{\phi} - \dot{\alpha})\\ &- (s\cos\alpha + l\cos\psi\sin\phi)(\dot{\theta} - \dot{\alpha}) + \dot{R}]\cdot\boldsymbol{i}\\ &+ [\dot{l}\cos\psi\sin\phi - l\sin\psi\sin\phi\cdot\dot{\psi} + l\cos\psi\cos\phi\cdot(\dot{\phi} - \dot{\alpha})\\ &+ (s\sin\alpha - l\cos\psi\cos\phi)(\dot{\theta} - \dot{\alpha}) + R\dot{\theta}]\cdot\boldsymbol{j}\\ &+ (\dot{l}\sin\psi + l\cos\psi\cdot\dot{\psi})\cdot\boldsymbol{k}\end{aligned} \tag{9}$$

Then the kinetic energy of the subsatellite can be derived from the formula

$$T = \tfrac{1}{2}m_s\boldsymbol{V}_s\cdot\boldsymbol{V}_s \tag{10}$$

Similarly, we need to approximate the potential energy U of the subsatellite

$$U = -\frac{\mu m_s}{|\boldsymbol{R} + \boldsymbol{s} + \boldsymbol{l}|} \tag{11}$$

Considering that $s \ll R$, $s < l$, by Taylor expansion we obtain

$$\begin{aligned}U \approx -(\mu m_s/R)\big[&1 + (l/R)\cos\phi\cos\psi - \tfrac{1}{2}(l^2/R^2)\\ &+ \tfrac{3}{2}(l^2/R^2)\cos^2\phi\cos^2\psi + o(l^3/R^3)\big]\end{aligned} \tag{12}$$

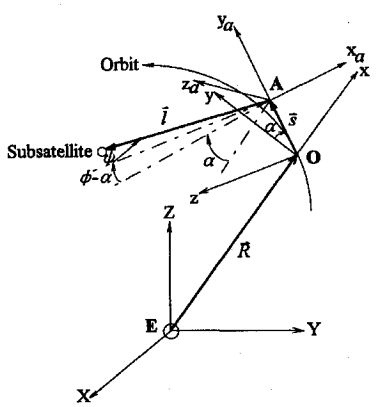

Fig. 3 Sketch of the development of the absolute velocity V_s of the subsatellite.

Therefore, by using the classical Lagrangian formulation

$$\frac{\mathrm{d}}{\mathrm{d}t}\left(\frac{\partial L}{\partial \dot{q}_i}\right) - \frac{\partial L}{\partial q_i} = Q_i \tag{13}$$

the following dynamical equations are obtained:

$$m_s\left\{\ddot{l} + s\cos\psi\cos(\phi-\alpha)\cdot(\ddot{\theta}-\ddot{\alpha}) + R\cos\psi\sin\phi\cdot\ddot{\theta} - \cos\psi\cos\phi\cdot\ddot{R} - l\dot{\psi}^2 - l\cos^2\psi(\dot{\phi}-\dot{\theta})^2 - s\cos\psi\sin(\phi-\alpha)\cdot(\dot{\theta}-\dot{\alpha})^2\right.$$
$$\left. + R\cos\psi\cos\phi\cdot\dot{\theta}^2 + 2\cos\psi\sin\phi\cdot\dot{R}\dot{\theta} - \frac{\mu[R\cos\phi - s\sin(\phi-\alpha)]\cos\psi - \mu l}{(R^2+s^2+2Rs\sin\alpha)^{\frac{3}{2}}} - \frac{3\mu l\cos^2\psi[R\cos\phi - s\sin(\phi-\alpha)]^2}{(R^2+s^2+2Rs\sin\alpha)^{\frac{5}{2}}}\right\} = Q_l$$

$$m_s\left\{l^2\cos^2\psi\cdot(\ddot{\phi}-\ddot{\alpha}) - l\cos\psi\cdot[s\sin(\phi-\alpha) + l\cos\psi](\ddot{\theta}-\ddot{\alpha}) + Rl\cos\psi\cos\phi\cdot\ddot{\theta} + l\cos\psi\sin\phi\cdot\ddot{R}\right.$$
$$- ls\cos\psi\cos(\phi-\alpha)\cdot(\dot{\theta}-\dot{\alpha})^2 - Rl\cos\psi\sin\phi\cdot\dot{\theta}^2 + 2l\cos^2\psi\cdot\dot{l}(\dot{\phi}-\dot{\theta}) - l^2\sin^2\psi\cdot\dot{\psi}(\dot{\phi}-\dot{\theta}) + 2l\cos\psi\cos\phi\cdot\dot{R}\dot{\theta}$$
$$\left. + \frac{\mu l[R\sin\phi + s\cos(\phi-\alpha)]\cos\psi}{(R^2+s^2+2Rs\sin\alpha)^{\frac{3}{2}}} + \frac{3}{2}\frac{\mu l^2\cos^2\psi\cdot[R^2\sin 2\phi + 2Rs\cos(2\phi-\alpha) - s^2\sin 2(\phi-\alpha)]}{(R^2+s^2+2Rs\sin\alpha)^{\frac{5}{2}}}\right\} = Q_\phi \tag{14}$$

$$m_s\left\{l^2\ddot{\psi} - ls\sin\psi\cos(\phi-\alpha)\cdot(\ddot{\theta}-\ddot{\alpha}) - Rl\sin\psi\sin\phi\cdot\ddot{\theta} + l\sin\psi\cos\phi\cdot\ddot{R} + l^2\cos\psi\sin\psi\cdot(\dot{\phi}-\dot{\theta})^2\right.$$
$$+ ls\sin\psi\sin(\phi-\alpha)\cdot(\dot{\theta}-\dot{\alpha})^2 - Rl\sin\psi\cos\phi\cdot\dot{\theta}^2 + 2l\dot{l}\dot{\psi} - 2l\sin\psi\sin\phi\cdot\dot{R}\dot{\theta}$$
$$\left. + \frac{\mu l[R\cos\phi - s\sin(\phi-\alpha)]\sin\psi}{(R^2+s^2+2Rs\sin\alpha)^{\frac{3}{2}}} + \frac{3\mu l^2\cos\psi\sin\psi\cdot[R\cos\phi - s\sin(\phi-\alpha)]^2}{(R^2+s^2+2Rs\sin\alpha)^{\frac{5}{2}}}\right\} = Q_\psi$$

where

$$Q_l = -\tau + \tfrac{1}{2}C_d\rho A[\dot{R}^2 + R^2(\dot{\theta} - a\sigma\sin\beta)^2$$
$$+ a^2\sigma^2R^2\cos^2\beta]^{\frac{1}{2}}[\dot{R}\cos\phi\cos\psi - R(\dot{\theta} - a\sigma\sin\beta)$$
$$\times\sin\phi\cos\psi - a\sigma R\cos\beta\sin\psi]$$
$$Q_\phi = -\tfrac{1}{2}C_d\rho Al[\dot{R}^2 + R^2(\dot{\theta} - a\sigma\sin\beta)^2 + a^2\sigma^2R^2\cos^2\beta]^{\frac{1}{2}}$$
$$\times[\dot{R}\sin\phi + R(\dot{\theta} - a\sigma\sin\beta)\cos\phi] \tag{15}$$
$$Q_\psi = -\tfrac{1}{2}C_d\rho Al[\dot{R}^2 + R^2(\dot{\theta} - a\sigma\sin\beta)^2 + a^2\sigma^2R^2\cos^2\beta]^{\frac{1}{2}}$$
$$\times[\dot{R}\cos\phi\sin\psi - R(\dot{\theta} - a\sigma\sin\beta)\sin\phi\sin\psi$$
$$+ a\sigma R\cos\beta\cos\psi]$$

Transforming the independent variable t into the true anomaly θ allows us to visualize the motion. It is easy to obtain

$$\dot{x} = x'E(\theta)$$
$$\ddot{x} = [x'' - x'F(\theta)]E^2(\theta) \tag{16}$$

where x represents the functions $l(t)$, $\phi(t)$, and $\psi(t)$, the dot and prime represent differentiation with respect to t and θ, respectively, and

$$E(\theta) = \omega(1-e^2)^{-\frac{3}{2}}(1+e\cos\theta)^2$$
$$F(\theta) = 2e\sin\theta\cdot G(\theta)$$
$$G(\theta) = \frac{1}{1+e\cos\theta} \tag{17}$$
$$\omega = \sqrt{\mu/a_0^3}$$

Theoretical Analysis

It is well known that

$$\sin x = x - (x^3/3!) + (x^5/5!) - \cdots$$
$$\cos x = 1 - (x^2/2!) + (x^4/4!) - \cdots \tag{18}$$

The number of terms on the right-hand side of the equations determines the degree of appoximation.

Simplest Case of Motion

If we take

$$s = 0, \qquad \alpha = 0, \qquad e = 0$$
$$\sin\phi = \phi, \qquad \sin\psi = \psi, \qquad \cos\phi = \cos\psi = 1 \tag{19}$$
$$R = R, \qquad \dot{\theta} = \omega, \qquad \theta = \omega t$$

Eqs. (14) and (15) are simplified to

$$l'' + 2l\phi' - 3l = Q_l^*$$
$$\phi'' + 2(l'/l)(\phi' - 1) + 3\phi = Q_\phi^* \tag{20}$$
$$\psi'' + 2(l'/l)\psi' + 4\psi = Q_\psi^*$$

where

$$Q_l^* = -\left(1/m_s\omega^2\right)\left\{\tau + \tfrac{1}{2}C_d\rho A[R^2(\omega - a\sigma\sin\beta)^2\right.$$
$$\left. + a^2\sigma^2R^2\cos^2\beta]^{\frac{1}{2}}[R(\omega - a\sigma\sin\beta)\phi + a\sigma R\cos\beta\cdot\psi]\right\}$$
$$Q_\phi^* = -\frac{C_d\rho A}{2lm_s\omega^2}[R^2(\omega - a\sigma\sin\beta)^2 + a^2\sigma^2R^2\cos^2\beta]^{\frac{1}{2}} \tag{21}$$
$$\times R(\omega - a\sigma\sin\beta)$$
$$Q_\psi^* = -\frac{C_d\rho A}{2lm_s\omega^2}[R^2(\omega - a\sigma\sin\beta)^2 + a^2\sigma^2R^2\cos^2\beta]^{\frac{1}{2}}$$
$$\times a\sigma R\cos\beta$$

Comparing Eq. (20) with Eq. (5) in Ref. 2, and considering that the positive directions of the in-plane and out-of-plane components are defined contrarily, we see that they are similar to each other.

When inclination of the orbit to the equatorial plane is equal to 0 deg, Eq. (6) becomes

$$a = 1 \qquad \alpha = 0\,\text{deg} \qquad \beta = 90\,\text{deg} \tag{22}$$

Then Eq. (21) can be replaced with the following equations:

$$Q_l^* = -\left(1/m_s\omega^2\right)\left[\tau + \tfrac{1}{2}C_d\rho AR^2(\omega-\sigma)^2\phi\right]$$

$$Q_\phi^* = -\frac{C_d\rho A}{2m_s\omega^2}R^2(\omega-\sigma)^2 \tag{23}$$

$$Q_\psi^* = 0$$

which shows that the air drag acts on the in-plane libration and keeps itself constant only if a (simplified) spherical atmosphere is adopted.

When $i = 90$ deg, the air drag will excite both the in-plane and the out-of-plane librations.

Case of Small Libration with Offset

If we take

$$s \neq 0$$

$$\sin\phi = \phi, \qquad \sin\psi = \psi \tag{24}$$

$$\cos\phi = 1, \qquad \cos\psi = 1$$

and neglect the small variables of higher order that combine librational angles and angular rates, Eqs. (14) and (15) are changed into the following equations:

$$\begin{aligned}
&\ddot{l} + 2l\dot{\phi}\dot{\theta} - 2(\mu/R^3)l - l\dot{\theta}^2 - s(\phi-\alpha)(\dot{\theta}-\dot{\alpha})^2 \\
&\quad = Q_{l2} - s(\ddot{\theta}-\ddot{\alpha}) \\
&\ddot{\phi} + 2(\dot{l}/l)(\dot{\phi}-\dot{\theta}) + (3\mu/R^3)\phi - (s/l)(\phi-\alpha)(\ddot{\theta}-\ddot{\alpha}) \\
&\quad -(s/l)(\dot{\theta}-\dot{\alpha})^2 = Q_{\phi 2} + \ddot{\theta} \\
&\ddot{\psi} + 2(\dot{l}/l)\dot{\psi} + (3\mu/R^3)\psi + \psi\dot{\theta}^2 - (s/l)\psi(\ddot{\theta}-\ddot{\alpha}) = Q_{\psi 2}
\end{aligned} \tag{25}$$

The offset s and the path angle α appear in every equation. If we let $s = s(t)$ and $\alpha = \alpha(t)$, then $s(t)$ and $\alpha(t)$ can be used as control variables; this technique is called offset control. Of course, several additional terms will appear in the dynamical equations in this case. Offset control makes it possible to retrieve the subsatellite quickly and stably within 1 km because the orders of magnitude of $l(t)$ and $s(t)$ will be comparable and the attitude motion of the system is affected by $s(t)$.

The term $\ddot{\theta}$ appears on the right-hand side of the second equation because the system moves in an elliptical orbit and this term excites the in-plane libration.

If the small terms of Eq. (18) on the right-hand side are retained in the second and the third orders, groups of more complicated equations are obtained. Coupling of the in-plane and out-of-plane librations arise from the second-order terms.

In addition, the effective area appears in each formula of the generalized forces. If the subsatellite is equipped with a sail and the projected area of the sail normal to the velocity $\boldsymbol{V}$ is adjusted, i.e., $A = A(t)$, then a new control strategy, which can be called air-drag control, may be developed.

Numerical Results

To show the influence of nonlinear terms and offset on the attitude motion, many numerical simulations have been run and comparisons have been made. The deployment and retrieval of a 150-kg subsatellite from the Space Shuttle at an apogee of 220 km was considered. The deploying strategy by Misra and Modi[11] and retrieval strategy by Xu et al.[15] were used. During deployment, the length of the tether changes from an initial value of 1 km to a final value of 100 km.

1) The deploying strategy is

$$l' = \begin{cases} cl & (0 < \theta < \theta_1) \\ cl_1 & (\theta_1 < \theta < \theta_2) \\ c(l_1 + l_2 - l) & (\theta > \theta_2) \end{cases} \tag{26}$$

Table 1 Symbols used in Figs. 4–12

Model	Symbol	Line style
Linear	+	
Second-order nonlinear	×	
Third-order nonlinear	Δ	
Without offset		Dashed
With offset		Solid

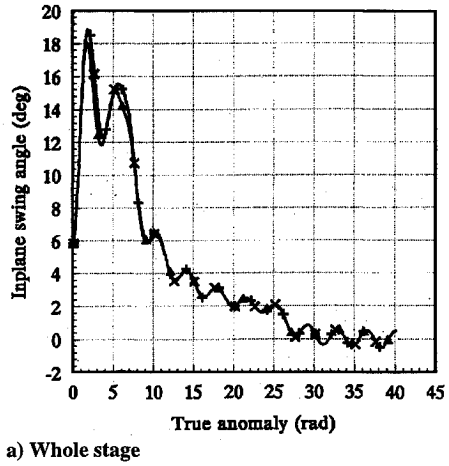

a) Whole stage

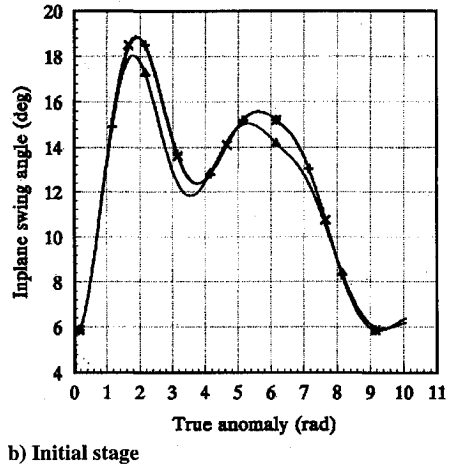

b) Initial stage

Fig. 4 Linear and nonlinear in-plane librations of the subsatellite during deployment.

where

$$\begin{aligned}
&\theta_1 = 2\pi, \qquad \theta_2 = 8\pi \\
&l_1 = l(\theta_1) \qquad l_2 = l(\theta_2) \qquad c = 0.38
\end{aligned} \tag{27}$$

2) The retrieval strategy is

$$l' = k_\theta(1 + k_l f)\left(1 - k_\phi f\phi' + k_f f\psi'^2\right) \qquad f = 1 - (l/l_m) \tag{28}$$

where

$$\begin{aligned}
&k_\theta = -\frac{c}{(1+e\cos\theta)^2(1-e^2)^{\frac{3}{2}}} \\
&c = 0.2, \qquad k_l = 2.0, \qquad k_\phi = 2.0 \\
&k_\psi = -9.0, \qquad l_m = 100\,\text{km}
\end{aligned} \tag{29}$$

Table 1 presents the symbols used in the following discussion. The contributions of the nonlinear terms of the second and third orders to the motion of the systems are shown in Figs. 4–9.

The results from Figs. 4–5 indicate that the second-order and third-order nonlinear terms only have a negligible influence on the initial in-plane libration of the subsatellite. The out-of-plane librations are approximately the same with or without nonlinear terms.

Figure 6 shows that nonlinear terms have changed the periodicity of the in-plane and out-of-plane libration unremarkably.

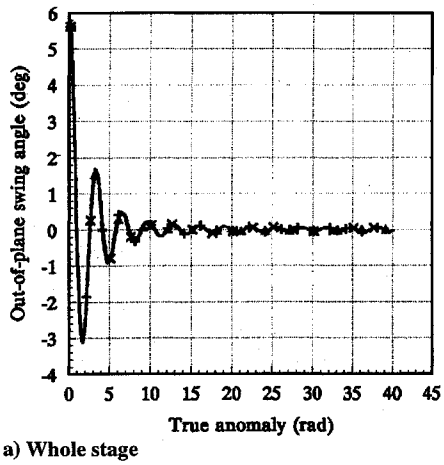

a) Whole stage

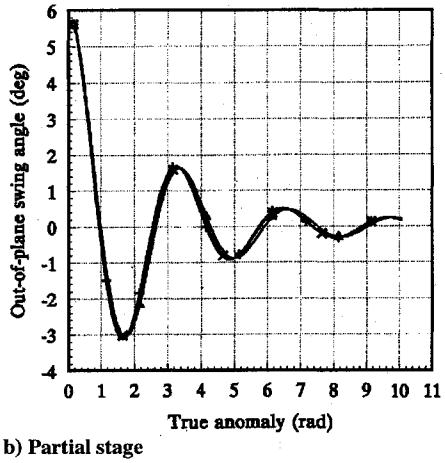

b) Partial stage

Fig. 5 Linear and nonlinear out-of-plane librations during deployment.

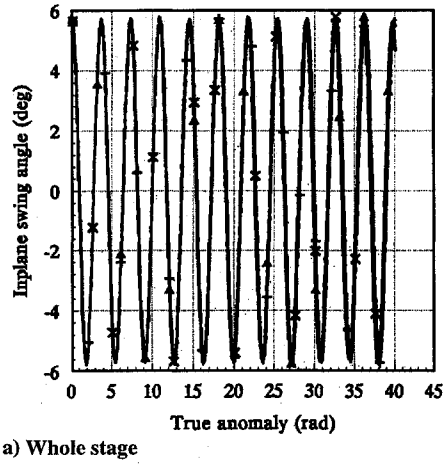

a) Whole stage

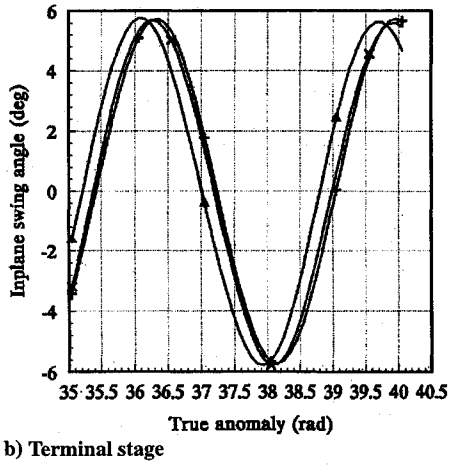

b) Terminal stage

Fig. 6 Linear and nonlinear in-plane librations during stationkeeping.

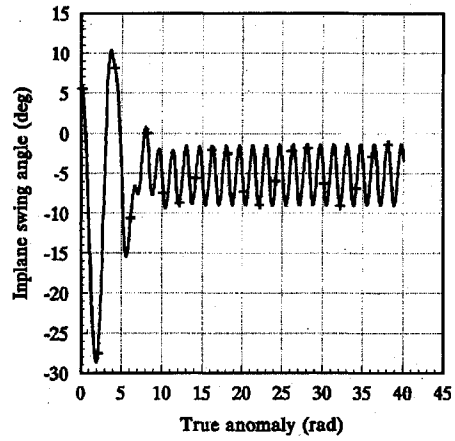

a) Linear model

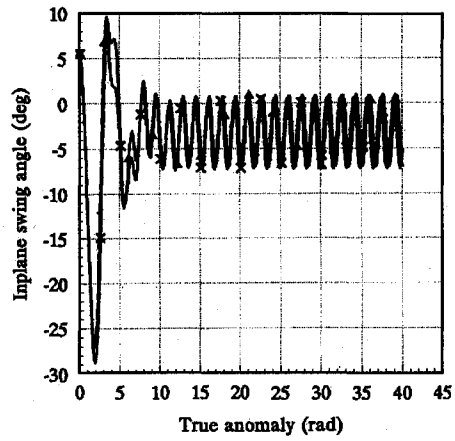

b) Nonlinear model

Fig. 7 Linear and nonlinear in-plane librations during retrieval.

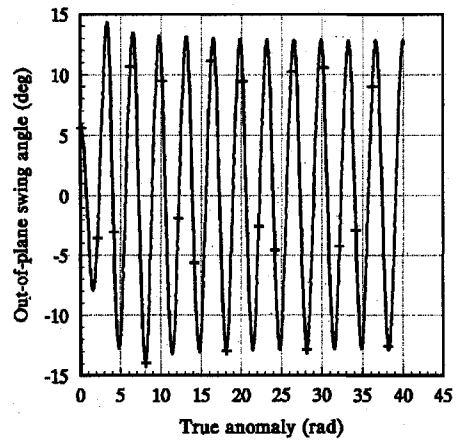

a) Linear model

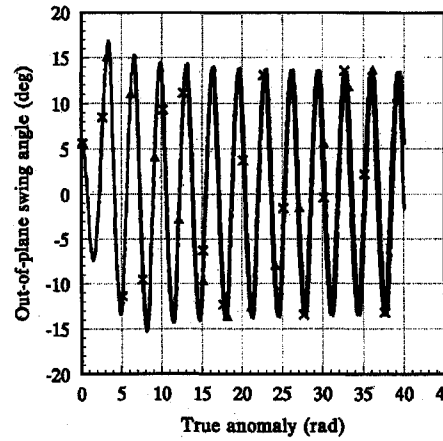

b) Nonlinear model

Fig. 8 Linear and nonlinear out-of-plane librations during retrieval.

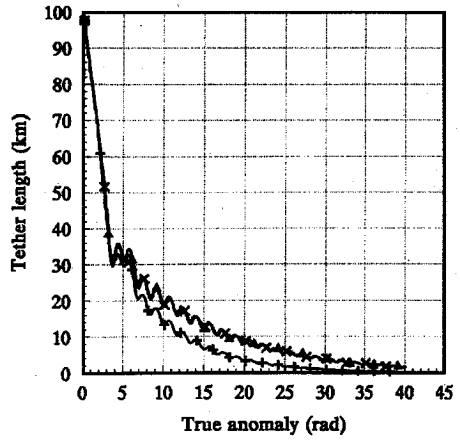

a) Whole stage

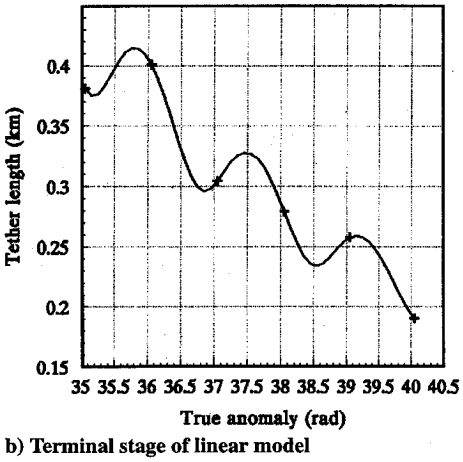

b) Terminal stage of linear model

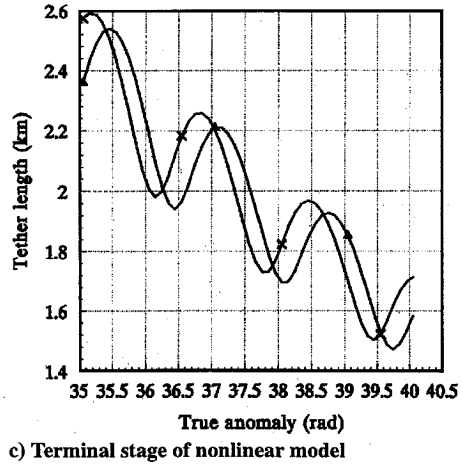

c) Terminal stage of nonlinear model

Fig. 9 Comparison of linear and nonlinear models with respect to length variation of the tether during retrieval.

The results from Figs. 7–9 make it clear that the introduction of nonlinear terms has a significant effect on the retrieval motion, especially on the in-plane libration, whose time history has noticeably shifted upward, and on the variation of the tether length l. It is difficult to retrieve the tether to within 1 km within acceptable time.

The effect of the offset s is shown in Figs. 10–12. The offset s is given the value 10 m in Figs. 10–11. Figure 10 indicates the effect of s on the linear model. Although s has almost no influence on the deployment motion, it greatly affects the in-plane libration during retrieval. From Fig. 10b, where the solid curve represents the case with offset $s = 10$ m, it is obvious that the linear model cannot be used for retrieval, especially considering the influence of the offset.

It is believed that the model in which the third-order nonlinear terms have been retained is close to the true conditions. Consequently, Fig. 11, where the solid curves represent the nonlinear model with $s = 10$ m and $e = 0$ and the dashed curves the nonlinear model without any offset, shows clearly that the offset has almost no influence on the motion of the subsatellite when

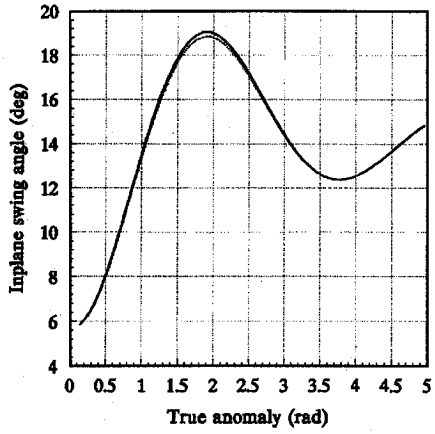

a) During deployment

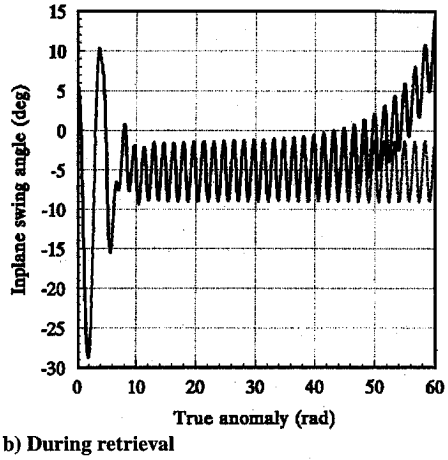

b) During retrieval

Fig. 10 In-plane librations of the linear model of the subsatellite with offset $s = 10$ m.

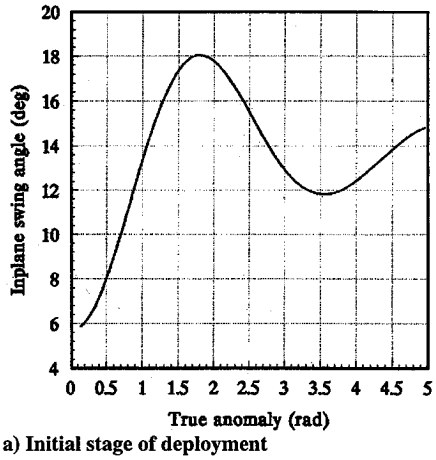

a) Initial stage of deployment

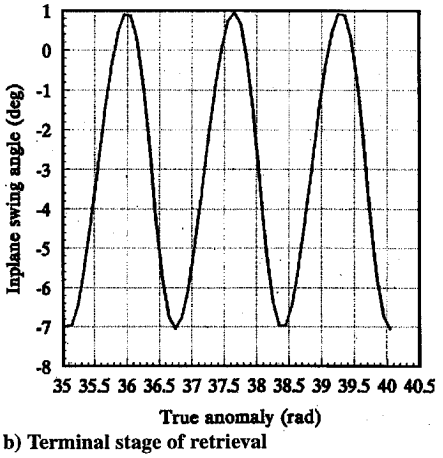

b) Terminal stage of retrieval

Fig. 11 In-plane librations of the third-order nonlinear model with $s = 10$ m and $e = 0$.

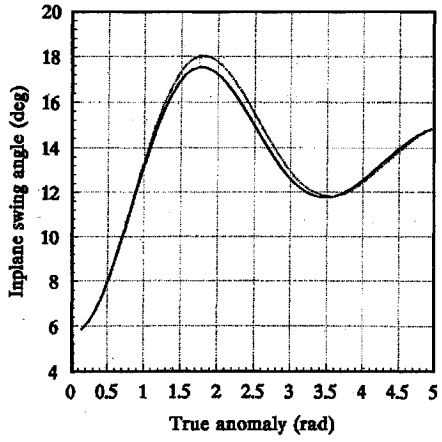

a) Initial stage of deployment

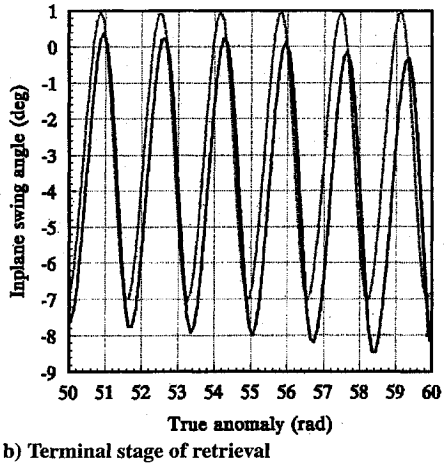

b) Terminal stage of retrieval

Fig. 12 In-plane librations of the third-order nonlinear model with $s = 0.001$.

the system moves in a circular orbit. Only when the offset is large enough and the system moves in an elliptical orbit can the influence of the offset be noticed, as Fig. 12 shows.

Figures 7–8 show that, with the preceding nonlinear retrieval strategy, the in-plane libration response is strongly dependent upon the model adopted, but the out-of-plane libration is not. To illustrate this interesting behavior, Eq. (20) can be written as

$$\begin{aligned} l'' + 2l\phi' - 3l &= Q_l^* \\ \phi'' + 2(l'/l)\phi' + 3\phi &= Q_\phi^* + 2(l'/l) \\ \psi'' + 2(l'/l)\psi' + 4\psi &= Q_\psi^* \end{aligned} \tag{30}$$

First, the retrieval strategy is strongly dependent on the state of the motion, and the states are relative to the model. Second, in the third equation here, the coefficient $2(l'/l)$ can be regarded as a damping factor. However, in the second equation of Eq. (30), it is not only a damping factor but also an excitation to the in-plane libration. Consequently, the retrieval strategy reacts to the in-plane libration more strongly than to the out-of-plane libration.

Conclusions

Nonlinear terms have negligible influence on the attitude motions of the subsatellite during deployment and stationkeeping; hence, linearization is feasible. During retrieval, the nonlinear terms affect the motion substantially. Consequently, when the initial amplitudes of the angles are not small, nonlinear models should be adopted. In general, the offset of the tether attachment to the Space Shuttle from the mass center of the system is an insignificant parameter. Nevertheless, with the linear model, the incorrect result that the offset affects the terminal phase of retrieval significantly will be obtained. In this case, only nonlinear models should be used.

References

[1]Misra, A. K., and Modi, V. J., "Dynamics and Control of Tether Connected Two-Body System—a Brief Review," International Astronautical Federation, IAF'82, Paris, Sept. 1982.

[2]Lorenzini, E. C., "A Three-Mass Tethered System for Micro-*g*/Variable-*g* Applications," *Journal of Guidance, Control, and Dynamics*, Vol. 10, No. 3, 1987, pp. 242–249.

[3]Anderson, J. L., "Outer Atmospheric Research Using Tethered Systems," *Journal of Spacecraft and Rockets*, Vol. 26, No. 2, 1989, pp. 66–71.

[4]Hurlbut, F. C., "Tether Satellite Potential for Rarefied Gas Aerodynamics Research," *Journal of Spacecraft and Rockets*, Vol. 26, No. 2, 1989, pp. 72–79.

[5]Webster, W. J., Jr., "Engineering Tethered Payloads for Magnetic and Plasma Observations in Low Orbit," *Journal of Spacecraft and Rockets*, Vol. 26, No. 2, 1989, pp. 80–84.

[6]Von Tiesenhausen, G., "Applications of Tethers in Space—a Review of Workshop Recommendations," NASA-TM-86549, May 1986.

[7]Buongiorno, C., and Vallerani, E., "Perspective Features of the Tethered Systems for Space Applications," International Astronautical Federation, 40th Congress, Oct. 1989.

[8]Banerjee, A. K., "Dynamics of Tethered Payloads with Development Rate Control," *Journal of Guidance, Control, and Dynamics*, Vol. 13, No. 4, 1990, pp. 759–762.

[9]Van der Ha, J. C., "Orbital and Relative Motion of a Tethered Satellite System," International Astronautical Federation, 34th Congress, IAF'83, Budapest, Hungary, Oct. 1983.

[10]Bainum, P. M., and Kumar, V. K., "Optimal Control of the Shuttle-Tethered- Subsatellite System," *Acta Astronautica*, Vol. 7, 1980, pp. 1333–1348.

[11]Misra, A. K., and Modi, V. J., "Dynamics of a Tether Connected Payload Deploying from the Space Shuttle," AIAA Paper 80-31693, April 1980.

[12]Ruying, F., and Bainum, P. M., "Dynamics and Control of a Space Platform with a Tethered Subsatellite," *Journal of Guidance, Control, and Dynamics*, Vol. 11, No. 4, 1988, pp. 377–380.

[13]Lakshmanan, P. K., Modi, V. J., and Misra, A. K., "Dynamics and Control of the Tethered Satellite System in the Presence of Offsets," *Acta Astronautica*, Vol. 19, No. 2, 1989, pp. 145–160.

[14]Soledov, A. B., *Handbook for Space Engineering*, Science Press, 1982, p. 32.

[15]Xu, D. M., Misra, A. K., and Modi, V. J., "Three-Dimensional Control of the Shuttle Supported Tethered Satellite Systems During Retrieval," AIAA Paper 83-45125, March 1983.

T. C. Lin
Associate Editor